Carbon Materials

DOI: 10.1002/anie.201209141

Small-Angle Neutron Scattering for In Situ Probing of Ion Adsorption Inside Micropores**

*S. Boukhalfa, L. He, Y. B. Melnichenko, and Gleb Yushin**

Transport and adsorption processes of electrolyte ions in porous carbon materials under an applied potential control the performance of double layer capacitors for rapidly emerging high-power energy storage applications,[1] capacitive deionization devices for water purification and desalination,[2] rotational motors for artificial muscles, microfluidic devices, and nanorobotics.[3]

Electrochemical analysis techniques combined with structural and chemical characterization of porous carbon materials offer limited prognostic abilities. Several studies revealed significant impact of structural defects in carbon materials on their electrosorption properties[4] and the enhanced ion adsorption in sub-nanometer pores[5] in selected materials systems. The observed phenomena, however, were not always confirmed in other carbon materials or electrolytes, and the universality of such observations remains a topic of debates in the scientific community. The challenge comes from the difficulty of independently tuning various material properties needed for systematic experimental studies and from the high complexity of realistic materials systems for ab initio simulations.

To gain better insights into adsorption phenomena, computer simulations were performed in model systems,[1a,6] with a stronger emphasis on ionic liquid (IL) electrolytes,[1a,6c–e] which do not contain solvent molecules and thus simplify the calculations. A recent study emphasized the importance of taking into consideration a more realistic structure of porous carbon materials.[7] While the obtained modeling results are insightful, development and adoption of complementary experimental techniques is critically needed to directly identify both the ion transport[8] and adsorption sites in a broad range of microporous solids as a function of the applied potential, verifying the molecular mechanisms previously proposed and providing guidance to future modeling efforts.

Recent studies have demonstrated that small-angle neutron scattering (SANS) can provide unique, pore-size-specific information on the adsorption of confined fluids and may be used to evaluate the density of the adsorbed molecules in nanometer and sub-nanometer pores.[9] In this work we report on the discovery of the unique capability of in situ SANS to directly visualize changes in the electrolyte ion concentration in pores of different sizes as a function of the potential applied to any nanoporous material. In contrast to prior studies,[5] the distribution of the ion density within the pores of different sizes can be measured within the same material. Since materials with different pore size distributions inevitably exhibit different microstructures and different concentrations of defects and surface functional groups, the proposed method offers the unique and important ability to study the effects of the pore size and surface chemistry independently.

The majority of electrolytes contain hydrogen atoms in either their solvent molecules or ions or both. We show that by monitoring changes in the distribution of the hydrogen atoms in the nanoconfined electrolyte upon the application of an external potential to porous carbon electrodes one can elucidate where the ion adsorption takes place. A simplified schematic of our experimental setup is shown in Figure 1. We

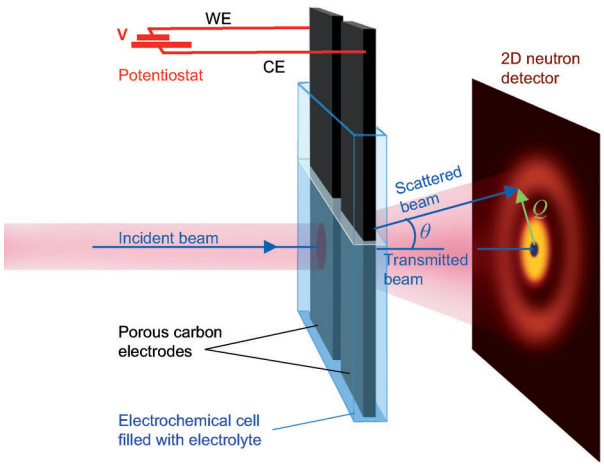

Figure 1. Experimental setup for in situ studies of ion adsorption on the surface of microporous carbon electrodes.

[*] S. Boukhalfa, Prof. G. Yushin
School of Materials Science and Engineering
Georgia Institute of Technology
Atlanta, GA (USA)
E-mail: yushin@gatech.edu
L. He, Y. B. Melnichenko
Neutron Sciences Directorate, Biology and Soft Matter Division
Oak Ridge National Laboratory, Oak Ridge, TN (USA)
Y. B. Melnichenko
Department of Physics and Astronomy
University of Tennessee, Knoxville, TN 37966 (USA)

[**] This work was partially supported by the Georgia Institute of Technology and the US Army Research Office (contract number W911NF-12-1-0259). The research at ORNL's High Flux Isotope Reactor was sponsored by the Laboratory Directed Research and Development Program and the Scientific User Facilities Division, Office of Basic Energy Sciences, U.S. Department of Energy. This research was also supported in part by the ORNL Postdoctoral Research Associates Program, administered jointly by the ORNL and the Oak Ridge Institute for Science and Education. We thank Micromeritics Inc. (US) and J. Jagiello for assistance with gas and vapor sorption analyses.

Supporting information for this article is available on the WWW under http://dx.doi.org/10.1002/anie.201209141.

used a microporous activated carbon fabric (ACF) as binder-free conductive electrodes for our studies (Figure S1 in the Supporting Information). In our proof-of-concept in situ SANS experiments we used aqueous electrolytes based on H_2SO_4 solutions in H_2O and D_2O. Our choice of electrolyte was motivated by a significant difference in the neutron scattering length density (SLD) of H_2O and C, and a small difference in the neutron SLD between D_2O and C.

Cyclic voltammetry (CV) studies performed in a symmetric two-electrode configuration in the voltage window between −0.6 and 0.6 V revealed nearly ideal capacitive behavior with a rectangular shape of the curves (Figure 2a,b and Figures S2 and S3). Analysis of the CV curves showed a noticeably higher ACF capacitance and a better capacitance retention in a H_2O-based electrolyte (Figure 2c and Figure S2c). The experimentally determined higher ionic conductivity of the H_2O-based electrolyte (Figure S4) may play a role in a better ACF capacitance retention (Figure 2c). A higher strength of the deuterium bonds over the hydrogen bonds[10] results in a higher viscosity of D_2O than H_2O[11] and contributes to a reduced overall mobility of the electrolyte ions.

In the absence of Faraday processes and for a similar ion surface density the carbon capacitance per unit surface area shall increase with decreasing average distance between the pore walls and the center of charge of the electrolyte ions near the surface. The size of the ion solvation shells in H_2O and D_2O is similar. At the same time, since D_2O is a weaker solvent, one may expect ions in D_2O to approach the oppositely charged pore walls closer because of the lower solvation energy and smaller free-energy barrier needed for the distortion of the solvation shell in this solvent. Because a small decrease in the carbon–ion charge separation leads to a large increase in the capacitance,[6b] one should expect ACF to exhibit a higher capacitance in a D_2O-based electrolyte (in contrast to our observations, Figure 2), if the average concentrations of electroadsorbed ions on the carbon surface were identical.

In situ SANS studies shed light on the origin of the unexpected performance. Under the application of a negative potential to an ACF working electrode (WE) in an aqueous H_2SO_4 solution, H-containing cations (such as H_3O^+, in the simplistic description) replace anions (such as HSO_4^- and SO_4^{2-}) and H_2O molecules, thereby increasing the concentration of H in the vicinity of the ACF surface and thus increasing the intensity of the scattered neutron beam and shifting the intensity curve up to higher values (Figure 3a). When a positive potential is applied to a working electrode, electrolyte anions replace both H-rich cations and H_2O molecules, thus decreasing the concentration of H atoms in the vicinity of the ACF surface and decreasing the scattering intensity (Figure 3a).

The application of a negative potential to an ACF working electrode in a H_2SO_4-containing D_2O solution increases the intensity of the scattered neutron beam more than in the other case because of a dramatically weaker scattering of neutrons from the deuterium atoms in D_2O (Figure 3b). Under the application of a positive potential to an ACF WE, the change in the H concentration becomes governed by the replacement of both cations (such as H^+, HD_2O^+) and D_2O solvent molecules by electrolyte anions (such as HSO_4^- and SO_4^{2-} ions in a simplistic case). The replacement of D_2O by SO_4^{2-} and of H^+ and HD_2O^+ by HSO_4^- are expected to have little impact on the scattering intensities. Because the replacement of HD_2O^+ and H^+ by $SO_4^{(2-)}$ contributes to a decrease of the H concentration in the ACF pores, whereas the replacement of D_2O by HSO_4^-, in contrast, leads to an increase in the H concentration, the change in the intensity of the scattered

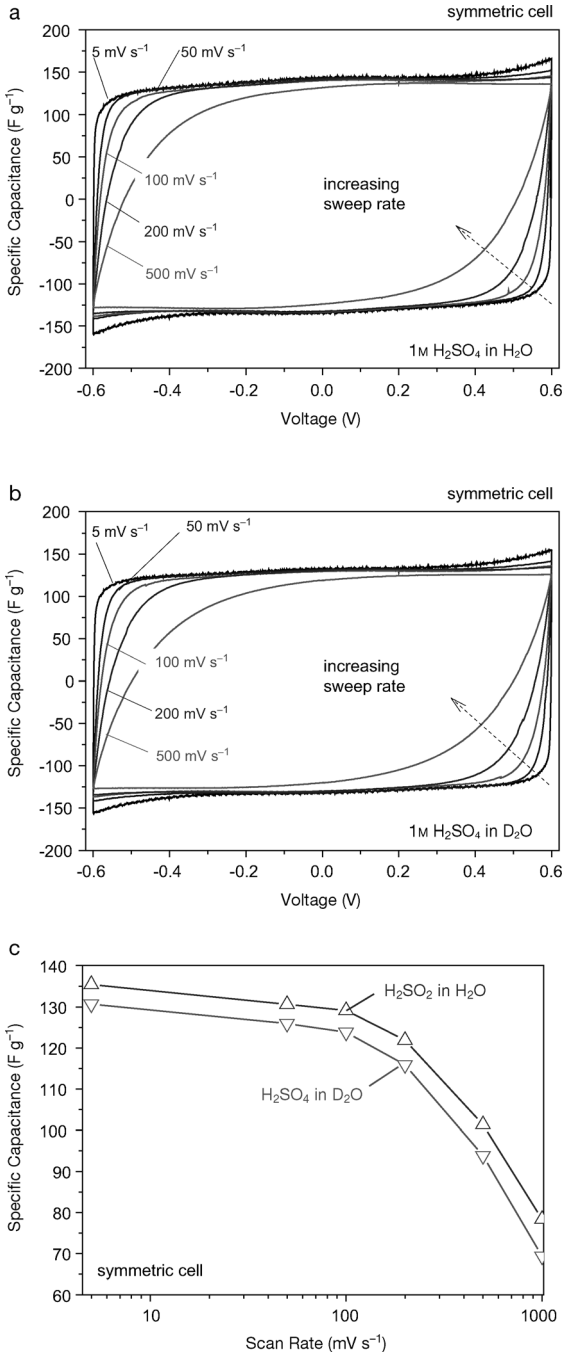

Figure 2. Electrochemical characterization of the activated carbon fabric in symmetric cells: cyclic voltammetry performed at different sweep rates in 1 M H_2SO_4 solution in a) H_2O and b) D_2O. c) Capacity retention as a function of the sweep rate.

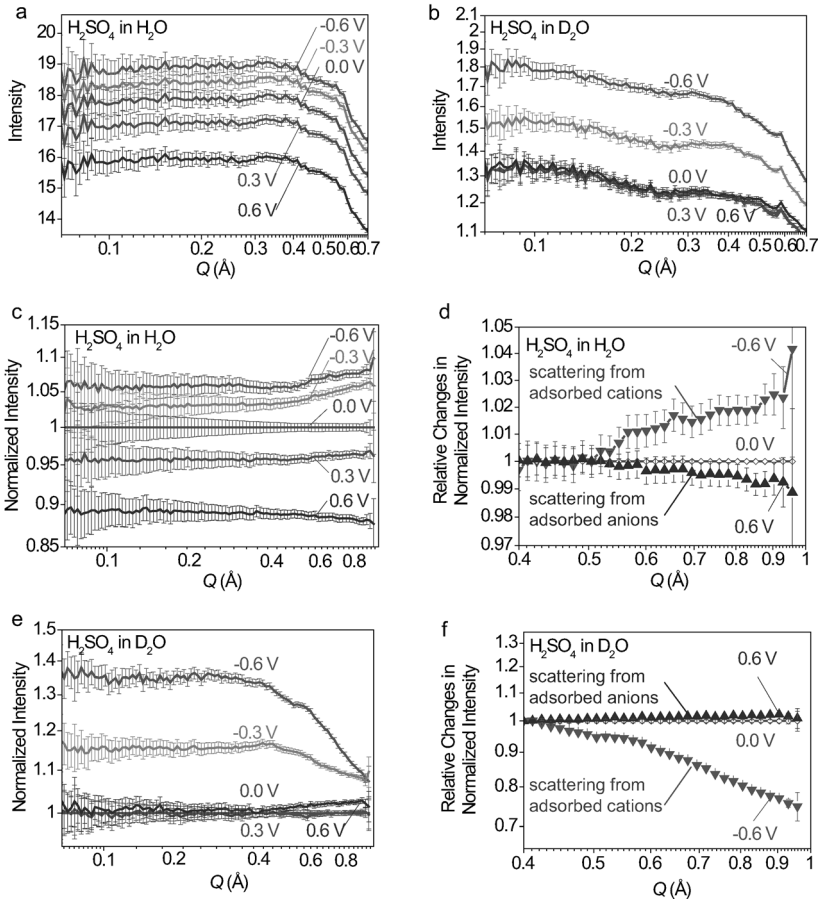

Figure 3. In situ neutron scattering experiments on ACF electrodes immersed into H_2O (a, c, and d) and D_2O-based (b, e, and f) electrolytes under application of a potential between the WE and CE: a and b) SANS patterns, c and e) SANS profiles normalized by the 0 V one, and d and f) relative changes in the intensity of the normalized SANS profiles.

beam is determined by the balance of both processes. In our case, we see minimal changes in the scattering intensity when the potential of the WE was increased from 0 to 0.6 V versus a counter electrode (CE) (Figure 3b).

To gain insights into the adsorption of ions within the pores of different sizes we normalized the SANS intensities to a zero-voltage SANS profile (Figure 3c,e). It is important to note that the variable scattering vector, Q, is inversely proportional to the pore size (large pores are present at small values of Q and vice-versa). In the case of the H_2O solvent, under the application of -0.6 V the scattering intensity increases by about 6% (Figure 3c), which represents a H enrichment of 6% within the relatively large pores. The smallest pores ($Q > 0.5$ Å^{-1}) of ACF exhibit an even higher ion adsorption capacity, as manifested by a higher H concentration in such pores at negative potentials and a lower H concentration at positive potentials.

The effect of the pore size on the ion electroadsorption can be seen more clearly in Figure 3d, where relative changes in the normalized scattering intensities are shown for both the negative and positive potentials applied to the ACF WE. Under the highest negative potential of -0.6 V the H enrichment remains constant for pores corresponding to $Q < 0.5$ Å^{-1} but increases in small pores corresponding to $Q > 0.5$ Å^{-1}. Under the highest positive potential of 0.6 V the H density decrease is enhanced in the smallest pores corresponding to the same Q (Figure 3d). Such observations support the recent hypotheses of the enhanced ion adsorption in the smallest pores.[5] In contrast to these prior studies, where the impact of the pore size was studied by analyzing completely different carbon materials exhibiting not only different pore size distributions but also different concentrations of defects and functional groups, our manuscript presents the first unambiguous observation of different ion adsorption in the smallest sub-nanometer pores.

In case of a D_2O solvent (Figure 3d,b,f), the negative polarization increases the neutron scattering intensity more dramatically because the scattering contrast between carbon and D_2O is much smaller than between carbon and H_2O. Under the application of -0.6 V the concentration of H increases by about 35% in large pores (Figure 3e). However, in sharp contrast to the H_2O solvent studies (Figure 3c,d), cation adsorption is significantly reduced in the smallest pores ($Q > 0.4$ Å^{-1}) in case of a D_2O solvent (Figure 4e,f).

The apparently smaller surface area of the ACF accessible to electrolyte ions explains the previously measured lower specific capacitance observed in a D_2O-based electrolyte (Figure 2c). If the energy of the solvent–pore wall interface could be neglected as traditionally assumed, the observed reduction of cation adsorption upon changing the solvent (compare Figure 3d,f) could not be explained, because the ion solvation energy is, in fact, smaller in D_2O than in H_2O and thus a distortion of the solvation shells and permeation of partially desolvated ions into the smallest pores should be easier in D_2O. Therefore, we postulate that D_2O–pore wall interactions obstruct ion access to a portion of the ACF surface. Such interactions should be greatly enhanced in the smallest pores, where interaction potentials of the solvent molecules with both sides of the pore walls overlap.[12] As a result, the relative concentration of ions becomes strongly reduced within sub-nanometer pores (Figure 3f).

Two separate scenarios may lead to the reduced accessible surface area of the ACF in the D_2O-based electrolyte: either the attraction of D_2O to the pore surface is so strong in the smallest pores that the replacement of the surface-adsorbed D_2O molecules by cations becomes energetically unfavorable or, in contrast, the hydrophobic carbon surface combined with the higher carbon/D_2O-based electrolyte interfacial energy prevents electrolyte access to the smallest pores. To identify which hypothesis is correct, we measured the relative degree of the ACF pore filling by both solvents and the relative

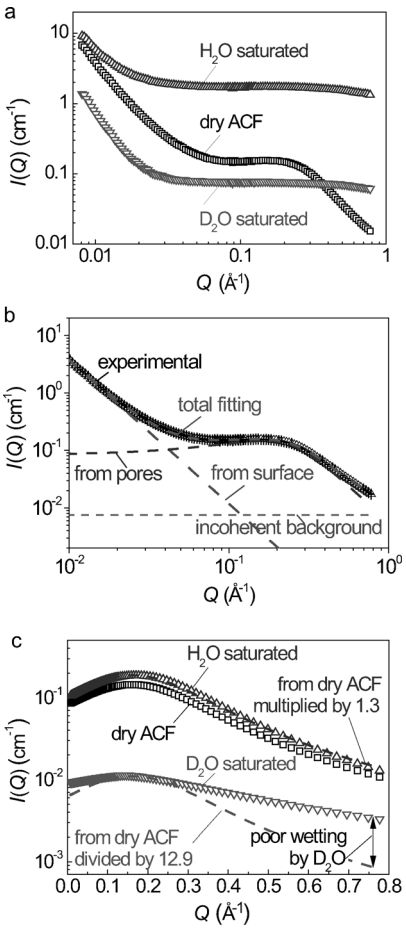

Figure 4. Neutron scattering experiments on dry ACF electrodes as well as on ACF immersed into H_2O and D_2O: a) SANS patterns. b) Deconvolution of the total scattering from dry ACF into scattering from the incoherent background, fiber surface, and pores. c) Neutron scattering from meso- and micropores in the studied samples. In (c) dashed lines represent scattering from dry ACF normalized to a maximum intensity of the neutron scattering curves of ACF immersed into two liquids: the red dashed line represents a normalization factor of 0.0775, and the blue dashed line represents a normalization factor of 1.3.

strength of the solvent–pore wall interactions. SANS performed on dry ACF and on ACF infiltrated with H_2O and D_2O media provided valuable insights (Figure 4). A negative SLD of H_2O ($-0.56\times10^{10}\,cm^{-2}$) increases the neutron contrast between carbon and H_2O saturated pores, leading to stronger scattering from H_2O-saturated ACF (Figure 4a). At the same time, a positive SLD of D_2O ($6.4\times10^{10}\,cm^{-2}$) being close to that of carbon ($4\times10^{10}\,cm^{-2}$) leads to a weaker scattering from D_2O-saturated ACF (Figure 4a). By deconvolution of the total scattering patterns (Figure 4a) into the scattering from the fiber outer surfaces, scattering from pores and incoherent background (see Figure 4b as an example) we could identify the degree of pore filling over a broad pore size range. The saturation of the ACF pores with H_2O leads to a parallel shift of the ACF scattering curve at all Q values with a factor of about 1.3 (Figure 4c), which is a ratio of the scattering intensities from H_2O-saturated and dry ACF at the value of the scattering vector corresponding to the maximum scattering intensity. This indicates that all the pores are evenly filled with H_2O. In contrast, saturation with D_2O leads to a Q-dependent decrease in the scattering intensity (Figure 4c), indicating that a significant portion of the smallest pores ($Q > 0.3\ Å^{-1}$) is not completely filled with D_2O. Vapor adsorption isotherms collected at 293 K (Figure S5) further confirm the SANS results. H_2O adsorption was observed at slightly lower relative pressures, indicating stronger interactions with carbon pore walls. More impressively, nearly $250\ cm^3\,g^{-1}$ less D_2O was adsorbed on the ACF surface at a relative pressure of 0.8 (Figure S5), indicating incomplete filling of pores by D_2O, as suggested by Figure 4c.

Since both SANS and sorption measurements indicate incomplete access of D_2O to the small pores, we conclude that the higher energy costs of maintaining a stronger deuterium bond network (compared to a hydrogen bond network) at the sub-nanometer proximity to the hydrophobic carbon surface is responsible for the formation of D_2O-based electrolyte depletion regions and for the dramatic difference between the electroadsorption of D_2O- and H_2O-based electrolyte ions in the smallest carbon nanopores.

We acknowledge that the idea that improved wetting properties may affect the specific capacitance of carbon is not new. Indeed prior studies reported a higher surface-area-normalized capacitance in porous carbon materials after surface oxidation, which improved the electrolyte wetting.[13] These and similar studies, however, did not take into consideration that the modification of the carbon surface chemistry likely increased the concentration of defects and opening of bottle-neck pores during oxidation may similarly increase the capacitance. Furthermore, no experimental studies have provided any insight on how the electrowetting phenomenon may counterbalance the insufficient carbon wetting by the solvent. As such, the impact of carbon wettability by the solvent on the specific capacitance has generated much controversy. In contrast, in our studies we unambigously show for the first time that the poor solvent wetting may indeed prevent electrolyte access to sub-nanometer pores even under the applied potential. More importantly, we demonstrate the capability of SANS to directly estimate the critical pore size, below which the inner surface area of carbon materials may not be accesible by electrolyte ions.

Multiple prior studies also observed a noticeable impact of organic electrolyte solvents on the carbon capacitance.[14] The majority of such studies focused on acetonitrile (AN) and propylene carbonate (PC) used in commercial electrochemical capacitors. While AN offers higher ionic conductivity and is more polar, it exhibits a nearly 45% lower dielectric constant than PC. Interestingly, in different porous carbon materials (and thus different pore size distributions and surface chemistries) the AN-based electrolytes inconsistently showed either higher[14a,b] or lower capacitance[14c] than PC-based electrolytes with an identical salt. In spite of the significant efforts, rather limited fundamental understanding of the solvent effects has gained so far. Our studies show a new route capable of demystifying the impact of the solvent and of revealing how the electrolyte–electrode interfacial

energy may have impact on the ion adsorption in pores of different sizes.

Finally, we would like to point out the unique capability of SANS to identify the degree of ion adsorption in pores of different sizes at no applied potential. This is an important question as the degree of pore filling affects the voltage dependence of the capacitance.[15] Several research groups suggested the opposite scenarios for the ion-filled small micropores. For example, Kiyohara et al.[16] suggest in their model that ions are expelled from small pores, when the porous electrode is not polarized. In contrast, Kondrat et al. assume the opposite based on the estimate of the role of image forces in the electrode that attract ions to electronically conductive pore walls.[17] By measuring lower neutron scattering intensity on an ACF electrode immersed in pure solvents than in electrolytes based on such solvents (Figure 5 a,b) we conclude that H-containing ions do enter the carbon pores without applied potential in case of both H_2O and D_2O solvents. More importantly, this H enrichment is stronger inside the smallest pores in both of these solvents (Figure 5 c).

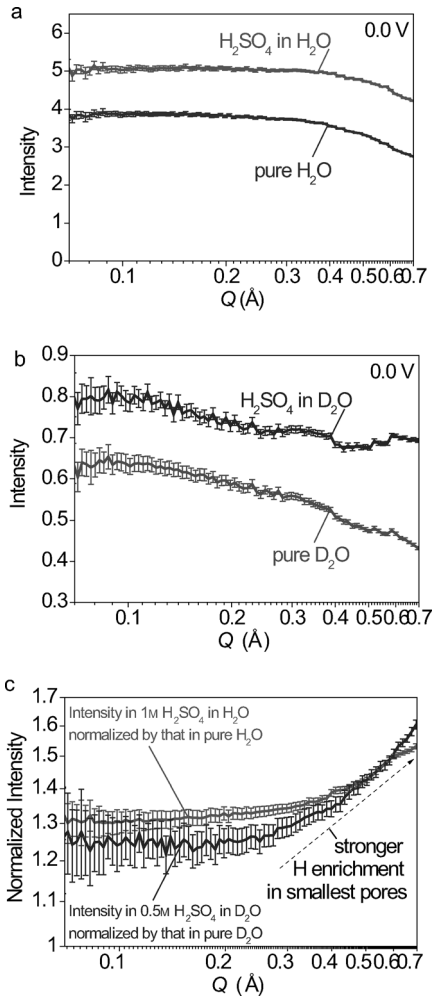

Figure 5. Neutron scattering experiments on ACF electrodes immersed into various liquids under no applied potential (0 V): a) SANS patterns on ACF in pure H_2O and 1 M aqueous H_2SO_4 electrolyte solution. b) SANS patterns on ACF in pure D_2O and 0.5 M H_2SO_4 electrolyte-containing D_2O solution. c) SANS profiles on ACF immersed into electrolyte solutions and normalized by the SANS profiles on ACF immersed into pure solvent (either H_2O or D_2O).

Received: November 14, 2012
Published online: February 12, 2013

Keywords: adsorption · carbon · energy storage · nanoporous materials · small-angle neutron scattering

[1] a) J. R. Miller, P. Simon, *Science* **2008**, *321*, 651 – 652; b) N. S. Choi, Z. H. Chen, S. A. Freunberger, X. L. Ji, Y. K. Sun, K. Amine, G. Yushin, L. F. Nazar, J. Cho, P. G. Bruce, *Angew. Chem.* **2012**, *124*, 10134 – 10166; *Angew. Chem. Int. Ed.* **2012**, *51*, 9994 – 10024.
[2] Y. Oren, *Desalination* **2008**, *228*, 10 – 29.
[3] J. Foroughi, G. M. Spinks, G. G. Wallace, J. Oh, M. E. Kozlov, S. L. Fang, T. Mirfakhrai, J. D. W. Madden, M. K. Shin, S. J. Kim, R. H. Baughman, *Science* **2011**, *334*, 494 – 497.
[4] C. Portet, G. Yushin, Y. Gogotsi, *Carbon* **2007**, *45*, 2511 – 2518.
[5] a) E. Raymundo-Piñero, K. Kierzek, J. Machnikowski, F. Beguin, *Carbon* **2006**, *44*, 2498 – 2507; b) J. Chmiola, G. Yushin, Y. Gogotsi, C. Portet, P. Simon, *Science* **2006**, *313*, 1760 – 1763; c) G. Salitra, A. Soffer, L. Eliad, Y. Cohen, D. Aurbach, *J. Electrochem. Soc.* **2000**, *147*, 2486 – 2493.
[6] a) G. Feng, R. Qiao, J. S. Huang, B. G. Sumpter, V. Meunier, *Acs Nano* **2010**, *4*, 2382 – 2390; b) J. S. Huang, B. G. Sumpter, V. Meunier, *Chem. Eur. J.* **2008**, *14*, 6614 – 6626; c) S. Boukhalfa, K. Evanoff, G. Yushin, *Energy Environ. Sci.* **2012**, *5*, 6872 – 6879; d) K. Evanoff, J. Khan, A. A. Balandin, A. Magasinski, W. J. Ready, T. F. Fuller, G. Yushin, *Adv. Mater.* **2012**, *24*, 533 – 0; e) J. Benson, S. Boukhalfa, A. Magasinski, A. Kvit, G. Yushin, *Acs Nano* **2012**, *6*, 118 – 125; f) L. Yang, B. H. Fishbine, A. Migliori, L. R. Pratt, *J. Am. Chem. Soc.* **2009**, *131*, 12373 – 12376.
[7] C. Merlet, B. Rotenberg, P. A. Madden, P.-L. Taberna, P. Simon, Y. Gogotsi, M. Salanne, *Nat. Mater.* **2012**, DOI: 10.1038/nman3260.
[8] M. D. Levi, G. Salitra, N. Levy, D. Aurbach, J. Maier, *Nat. Mater.* **2009**, *8*, 872 – 875.
[9] Y. B. Melnichenko, G. D. Wignall, *J. Appl. Phys.* **2008**, *103*, 039902.
[10] S. Scheiner, M. Cuma, *J. Am. Chem. Soc.* **1996**, *118*, 1511 – 1521.
[11] F. J. Millero, R. Dexter, E. Hoff, *J. Chem. Eng. Data* **1971**, *16*, 85 – 87.
[12] R. T. Yang, *Adsorbents: Fundamentals and Applications*, Wiley, Hoboken, **2003**.
[13] S. J. Kim, S. W. Hwang, S. H. Hyun, *J. Mater. Sci.* **2005**, *40*, 725 – 731.
[14] a) M. Arulepp, L. Permann, J. Leis, A. Perkson, K. Rumma, A. Janes, E. Lust, *J. Power Sources* **2004**, *133*, 320 – 328; b) H. Tamai, M. Kunihiro, M. Morita, H. Yasuda, *J. Mater. Sci.* **2005**, *40*, 3703 – 3707; c) R. Kötz, M. Hahn, R. Gallay, *J. Power Sources* **2006**, *154*, 550 – 555.
[15] M. V. Fedorov, N. Georgi, A. A. Kornyshev, *Electrochem. Commun.* **2010**, *12*, 296 – 299.
[16] K. Kiyohara, T. Sugino, K. Asaka, *J. Chem. Phys.* **2010**, *132*, 144705.
[17] S. Kondrat, N. Georgi, M. V. Fedorov, A. A. Kornyshev, *Phys. Chem. Chem. Phys.* **2011**, *13*, 11359 – 11366.
[18] J. Jagiello, *Langmuir* **1994**, *10*, 2778 – 2785.

